A Magnetic Particle Imaging (MPI) simulation for scaling from rodent to human

MGH/HST Athinoula A. Martinos Center for Biomedical Imaging
MASSACHUSETTS GENERAL HOSPITAL | Harvard-MIT Health Sciences & Technology
Massachusetts Institute of Technology

Erica E. Mason[1,3], Clarissa Z. Cooley[1], Stephen F. Cauley[1], Lawrence L. Wald[1,2]
MGH/HST A.A. Martinos Center for Biomedical Imaging, Massachusetts General Hospital[1], Harvard Medical School[2], and Harvard-MIT Health Sciences & Technology[3].

Background

Magnetic Particle Imaging (MPI) is a tracer-based imaging technology introduced in 2005[1] that detects the concentration of injected superparamagnetic iron oxide nanoparticles (SPIONs) using their nonlinear magnetic response. The higher order harmonics in the signal produced by SPION magnetization indicates their presence (Fig. 1a), and by selective saturation, the nonlinear signal can be localized and mapped to form an image of the distribution (Fig. 1b).

Due to the strong magnetic moment of SPIONs and zero-background signal, MPI has the potential to have a significant improvement in sensitivity over SPION detection with MRI. To date, rodent-sized MPI scanners exist[2], [3], but MPI has not been scaled for use on humans. Several barriers exist to increasing the scanner size, and the effect of this scaling on spatial resolution and sensitivity are only in the initial stages of investigation[4], [5].

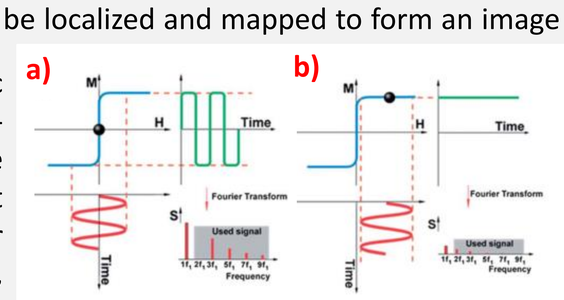

Figure 1. [1] a) Langevin response M(H) produces square wave signal, which includes higher order harmonics of the drive frequency. b) Driven in the saturation regime, the nonlinear signal is masked.

MPI signal and image simulation tools are needed to examine the sensitivity and spatial resolution tradeoffs of larger scanner configurations and to provide the equivalent of coil sensitivity maps to assess the potential of using array detectors in MPI for improving image localization. These simulations utilize electromagnetic models of the required drive, gradient and shift fields as well as the Faraday detector geometries used to measure the signal. Others have developed dedicated simulation tools for various aspects of the MPI scanner[4], [6]. Here, we focus on the localized sensitivity profiles of human-sized multichannel detectors.

MPI System Setup

A Biot-Savart magnetic field calculation of arbitrary coil windings has been implemented in MATLAB over the imaging FOV. The simulated drive, gradient and shift fields provide the input to calculating the SPION magnetization, **M**(**r**,t), based on the SPION-specific Langevin curve. The signal voltage is calculated by Eq. 1, where $\mathbf{B_1}(\mathbf{r})$ is the field produced per unit current by the receive coil, which is related through reciprocity to the detection efficiency via the dot product of $\mathbf{B_1}(\mathbf{r})$ with the temporal derivative of the SPION magnetization.

$$v(t) = -\mu_0 \int \mathbf{B_1}(\mathbf{r}) \cdot \frac{\partial}{\partial t}\mathbf{M}(\mathbf{r},t) d^3r \qquad (1)$$

For projection reconstruction imaging with a 2D field-free line (FFL) using the coordinate system defined in Fig. 2, we follow the basic methodology outline of Goodwill et al.[7] with the exception that we use a simulated shift field which is a step function instead of a ramp. This eliminates the need for gridding or a velocity normalization since the shift field is constant during the measurement of each point in a projection. Preamp noise is approximated by addition of $4\ \mathrm{nV}/\sqrt{\mathrm{Hz}}$ white Gaussian noise. A projection is formed by using the shift fields to sweep the FFL across the FOV along x'. The process is repeated at different projection angles and for different z offsets to form a stack of 2D images as in CT.

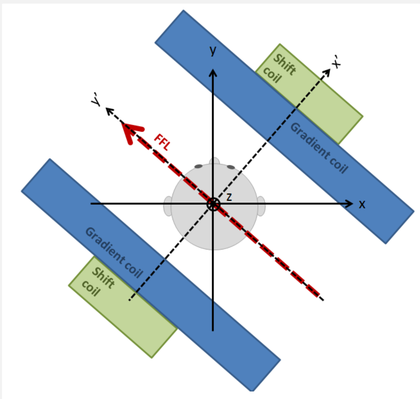

Figure 2. Definition of the coordinate system appropriate for 2D projection-based MPI. The x,y,z coordinates are patient-centric. The FFL is always along y' which is rotated with respect to the patient. The shift fields always shift the FFL along x' (also rotated with respect to the patient). The drive field is applied along z.

The simulation can be used to interrogate multiple aspects of MPI systems. To examine the spatial variation of detectors' sensitivity, we form **detection sensitivity maps** (see Figs. 3 + 4). To create point spread functions to investigate spatial resolution, we form **sensitivity projection functions**, which can be used to reconstruct images via filtered back-projection or iterative minimization methods (see Fig. 5 + 6).

For any of these simulation outputs, a choice can be made about which temporal components of the induced magnetization are considered. All temporal components (those at the drive frequency and all its harmonics), only a subset of these frequencies, such as only the 3rd harmonic, or only the higher harmonics (omitting the drive frequency response) can be used.. These different choices are informative since detection strategies are forced to filter out the magnetization's response at the drive frequency.

Simulation Results

Detection sensitivity maps:

To create detection sensitivity maps, we integrate (as in Eq. 1) for a given point source while applying only the drive field. The point source is moved voxel-by-voxel and this integral repeated for each to form the 2D map.

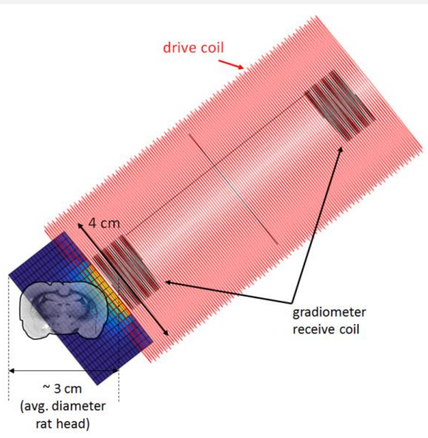

Figure 3. A single-sided rodent MPI detector (drive coil + gradiometer receive coil) for functional MPI experiments and its detection sensitivity map outside of the detector. The map shows amplitude measurements of the 3rd harmonic component for a point source moved to each voxel. The detection sensitivity map is overlaid with a rat brain image. The FOV is 4 x 4 x 2 cm on a 21 x 21 x 21 grid.

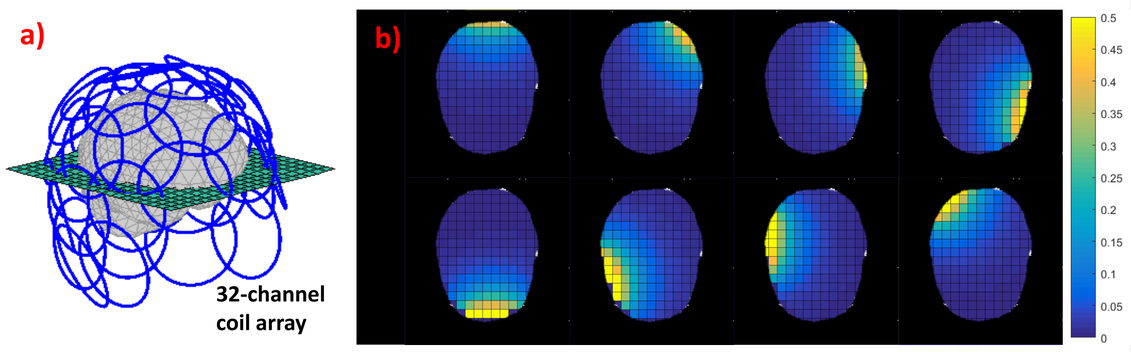

Figure 4. a) Geometry of a 32-channel head coil array with brain mesh (adapted from a 32-channel MRI head coil design[8], and b) localized MPI detection sensitivity maps for 8 of the 32 channels in the array. These are used to investigate encoding techniques for parallel imaging with partial FOV projections. Map shows amplitude measurements of the 3rd harmonic component of the signal voltage for a point source moved to each voxel. Amplitudes normalized and shown for z=0 axial slice. FOV is 24 x 24 x 12.4 cm on a 20 x 20 x 5 grid.

Sensitivity projection functions and reconstructed images:

A sensitivity projection function is formed by applying an FFL and integrating Eq. 1 for discrete shifts of the FFL along x'. Projection functions from multiple angles of a given z location can be used to reconstruct an image of an axial slice of the region.

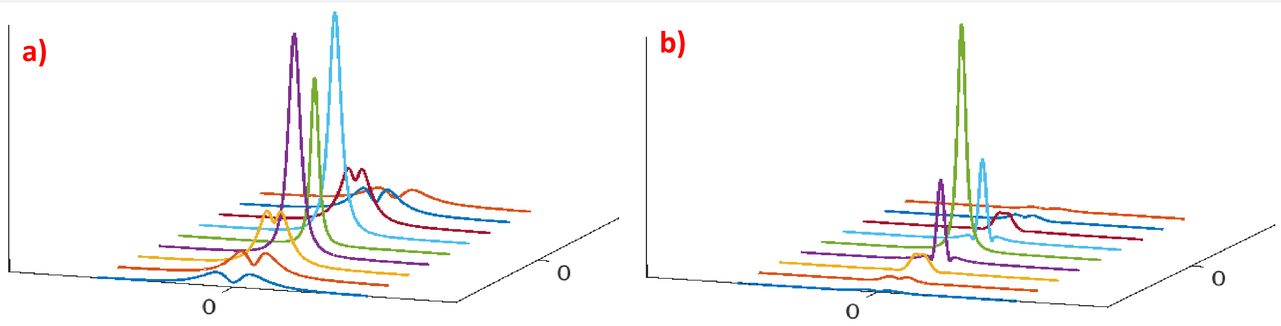

Figure 5. 1D sensitivity projection functions for a point source for 9 z locations of the point source spaced by 5mm. Projection axis gridded into 240 points spanning 240mm. Modeled point source represents 50ng of SPIONs. FFL gradient strength is 5T/m. 20mT 10kHz sinusoidal drive field in the z direction. Signal plotted is a) root mean square of the signal voltage with the drive frequency filtered out, and b) amplitude of only the 3rd harmonic component of the signal voltage.

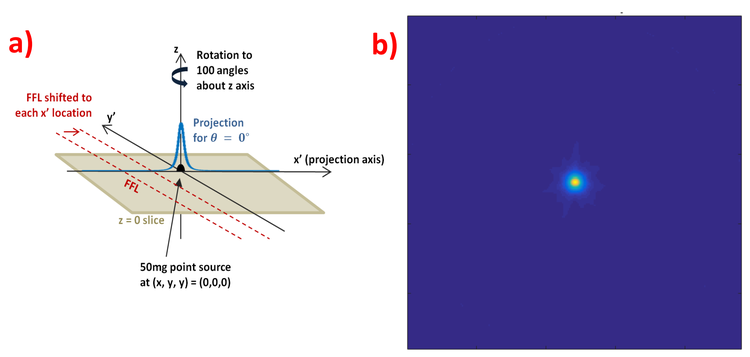

Figure 6. a) Geometry for producing sensitivity projection functions, used to reconstruct b) 2D image of the z = 0 axial slice. 100 evenly-spaced angles from 0 to π are used. The simulated point source represents 50mg at the isocenter in a $12.55\mathrm{mm}^3$ voxel. The projection axis is gridded into 240 points spanning 240mm. The FFL gradient strength is 5T/m in both x' and z directions. The drive field is a 20mT sinusoid oscillating in the z direction at 10kHz, and is shifted to each x' location. The FWHM of the signal is 7.1mm and the image has signal-to-noise ratio of 1.35×10^3.

Conclusion

The simulation tool we present allows us to generate localized MPI sensitivity maps and projection functions for different coil geometries and applications, providing the means to explore additional encoding schemes in MPI. These examples demonstrate the simulation tool's utility for innovating new parallel imaging techniques in MPI and examining image quality when MPI is scaled to human size.

Acknowledgements

Technical assistance from groups of S. Conolly, UC Berkeley, and M. Griswold, Case Western.

Funding

This work is funded by NIMH R24 106053, and supported by the NSF GRFP under Grant No. (1122374) and by the Martinos Center AMNTP NIH T90DA022759/R90DA023427.

References

[1] Gleich et al. Nature. 2005. [2] Goodwill et al. Rev. Sci. Instrum. 2012. [3] Weber et al. Biomed. Eng. 2013. [4] Bringout et al. IWMPI 2015 5th Int. Work. 2015. [5] Borgert et al. Biomed. Tech. 2013. [6] Weizenecker et al. Phys. Med. Biol. 2007. [7] Goodwill et al. *IEEE Trans. Med. Imag.*2012. [8] Lin. http://maki.bme.ntu.edu.tw